European Journal of Pharmaceutics and Biopharmaceutics 89 (2015) 300–311

Contents lists available at ScienceDirect

European Journal of Pharmaceutics and Biopharmaceutics

journal homepage: www.elsevier.com/locate/ejpb

Research paper

Stealth anti-CD4 conjugated immunoliposomes with dual antiretroviral drugs – Modern Trojan horses to combat HIV

Lakshmi Narashimhan Ramana [a], Shilpee Sharma [b], Swaminathan Sethuraman [a], Udaykumar Ranga [b], Uma Maheswari Krishnan [a,*]

[a] Centre for Nanotechnology & Advanced Biomaterials (CeNTAB), SASTRA University, Thanjavur, India
[b] HIV–AIDS Laboratory, Molecular Biology and Genetics Unit, Jawaharlal Nehru Centre for Advanced Scientific Research (JNCASR), Bangalore, India

ARTICLE INFO

Article history:
Received 19 May 2014
Accepted in revised form 25 November 2014
Available online 12 December 2014

Keywords:
Dual drug loaded anti-CD4 conjugated
anti-CD4 conjugated immunoliposomes
Anti-CD4
Nevirapine
Saquinavir
HIV
Targeting
Viral load

ABSTRACT

Highly active antiretroviral therapy (HAART) is the currently employed therapeutic intervention against AIDS where a drug combination is used to reduce the viral load. The present work envisages the development of a stealth anti-CD4 conjugated immunoliposomes containing two anti-retroviral drugs (nevirapine and saquinavir) that can selectively home into HIV infected cells through the CD4 receptor. The nanocarrier was characterized using transmission electron microscopy, FTIR, differential scanning calorimetry, particle size and zeta potential. The cell uptake was also evaluated qualitatively using confocal microscopy and quantitatively by flow cytometry. The drug to lipid composition was optimized for maximum encapsulation of the two drugs. Both drugs were found to localize in different regions of the liposome. The release of the reverse transcriptase inhibitor was dominant during the early phases of the release while in the later phases, the protease inhibitor is the major constituent released. The drugs delivered via anti-CD4 conjugated immunoliposomes inhibited viral proliferation at a significantly lower concentration as compared to free drugs. *In vitro* studies of nevirapine to saquinavir combination at a ratio of 6.2:5 and a concentration as low as 5 ng/mL efficiently blocked viral proliferation suggesting that co-delivery of anti-retroviral drugs holds a greater promise for efficient management of HIV-1 infection.

1. Introduction

Acquired immune deficiency syndrome (AIDS), caused by the human immunodeficiency virus (HIV), presents a huge challenge for treatment as it tends to disable the immune system thereby leaving the patient susceptible to many opportunistic infections [1]. According to the 2013 WHO report, about 34 million people have been diagnosed to be HIV positive throughout the world [2]. Highly active retroviral therapy (HAART) is one of the treatment strategies currently employed for treatment of HIV infections where a cocktail of drugs, each active at different stages of the disease, is administered to the patient [3]. However, HAART therapy has not proved very effective and is severely limited due to various factors. Most of the conventional HAART drugs produce various adverse effects such as skin rashes, vomiting, diarrhea and liver disorders [4].

Systemic administration of combinations of various drugs may also result in enhanced elimination of one drug with respect to the other leading to poor bioavailability of drug(s) in the combination. For instance, it has been demonstrated that when the two drugs nevirapine and saquinavir are administered in tandem, selective metabolization of saquinavir is promoted due to the activation of the cytochrome enzyme CYP3A4 [5]. This reduces the bioavailability of saquinavir and necessitates higher dosage of the drug thereby amplifying the possibility of adverse effects [6]. This problem can be circumvented if both drugs are made available to the target cell simultaneously. Administration of higher doses of the drugs in the conventional therapy may evoke the drug resistance mechanism thus lowering the therapeutic efficacy [7]. In addition, most drugs suffer from poor bioavailability due to metabolization or rapid elimination and hence the amount of drug reaching the target CD4 positive cells is inadequate [8]. Currently, frequent doses are administered to counter this effect, but these results in higher levels of adverse effects. Most of the drugs used in HAART are unable to cross the blood–brain barrier and therefore could not annihilate the HIV virions residing in the glial cells of the brain [9]. These disadvantages of the conventional therapy can be overcome by specifically targeting virus-infected cells.

The advent of nanotechnology has opened new vistas in chemotherapeutics by imparting target specificity and enhanced

* Corresponding author. Departments of Chemistry, Bioengineering & Pharmacy, Centre for Nanotechnology & Advanced Biomaterials (CeNTAB), School of Chemical & Biotechnology, SASTRA University, Thanjavur 613 401, Tamil Nadu, India. Tel.: +91 4362 264101x3677; fax: +91 4362 264120.
E-mail address: umakrishnan@sastra.edu (U.M. Krishnan).

http://dx.doi.org/10.1016/j.ejpb.2014.11.021
0939-6411/

therapeutic dosages to the target site. This can result in reduced frequency of administration and side effects while improving bioavailability and therapeutic efficacy. Many attempts have been made to improve the bioavailability of drugs through the use of nanocarriers [10]. A wide range of nanocarriers has been investigated for site-specific delivery of anti-cancer agents and antimicrobial agents [11]. However, not much focus has been directed toward site-specific delivery of anti-retrovirals. Some of the nanocarriers that have been explored for delivery of anti-retroviral drugs are liposomes [12], dendrimers [13], solid lipid nanoparticles [14], chitosan nanoparticles [15] and polymeric nanoparticles [6]. Most of these carriers have been developed for monotherapy i.e., treatment with a single drug. Combinational therapy employing nanocarriers has been reported for PLGA nanoparticles containing ritonavir, efavirenz and lopinavir [16]. A PLGA-based vaginal gel with raltegravir and efavirenz has also been reported [17]. No other reports are available in the context of multiple drug-loaded carriers for treatment of HIV infections.

HAART alone is not solely efficient for the treatment of the HIV because there are other opportunistic infections like histoplasmosis, Kaposi's sarcoma, tuberculosis, and pneumonia that accompany HIV infections due to the decrease in the number of the CD4 positive immune cells. Treatment with liposomal doxorubicin has been employed for reducing the tumor progression in HIV-associated Kaposi's sarcoma, which is currently in the phase II clinical trials [18]. Thus a combined therapy of HAART drugs and other drugs are used for the treatment of HIV infections in conventional therapy. However, effective reduction in the viral load may reduce the risk of development of such opportunistic infections thereby decreasing the need for other types of drugs along with HAART emphasizing the need for development of efficient anti-HIV strategies. Use of targeted nano-carriers containing co-encapsulated anti-retroviral drugs may improve treatment outcomes. However, this facet remains relatively unexplored.

Targeting of the liposomal system to the virus infected cells is a key requisite to ensure undesirable interactions resulting in the loss of efficacy as well as to minimize adverse effects. Many strategies have been attempted to specifically target virus-infected cells. These include conjugation of specific ligands to bind to gp120 in the HIV [19], glycan residues in the viral envelope [20], CXCR4 in the T cells [21], CCR5 in the macrophages, T cells and dendritic cells, HLA receptors in the virus infected cells [22], tuftsin receptors in the macrophages [23], CD4 receptors of both T cells and macrophages [24–27], etc. However, each strategy has met with limited success owing to various factors.

The present study aims to develop a liposomal delivery system encapsulating two drugs. The drugs chosen for the study are a reverse transcriptase inhibitor (nevirapine) that is active in the early life cycle of the HIV life cycle [28] and the protease inhibitor (saquinavir) that is more effective during the late phase of the HIV life cycle [29]. The difference in the hydrophobicity of both drugs is expected to influence their localization within the liposomes and consequently their release profiles. Target-specificity is achieved by introducing an anti-CD4 moiety on the surface of the liposomes to specifically home into cells that are commonly infected with HIV. The antibody employed in the present work is expected to target to both CD4 positive T_H (helper T) cells and also the macrophages, which are the primary hoarding cells for HIV and hence can provide better therapeutic benefits.

2. Materials and methods

2.1. Materials

Sodium dihydrogen phosphate, disodium hydrogen phosphate and HEPES (hydroxyethylpiparazinyl ethane sulfonic acid) were purchased from Merck Chemicals, India. Saquinavir was a kind gift from M/s Hetero drugs, India and nevirapine was a kind gift from M/s Boehringer Ingelheim Ltd., Germany. RPMI 1640 medium was procured from Sigma–Aldrich, USA and CellTiter 96®AQueous one solution was purchased from Promega, USA. Dulbecco's modified Eagle's medium (Sigma–Aldrich, USA), fetal bovine serum (Biological Industries, Israel) were also used in the study. Egg phosphatidyl choline (Egg PC), distearoylphosphatidylethanolamine–poly(ethylene glycol) (DSPE–PEG), NBD-DPPE (1,2-dipalmitoyl-sn-glycero-3-phosphoethanolamine-N-(7-nitro-2-1, 3-benzoxadiazol-4-yl) [Triethylamine salt] and maleimide-terminated DSPE–PEG (DSPE–PEG-mal) were purchased from NOF, Japan while cholesterol was procured from Sigma–Aldrich, USA. The anti-CD4 antibody purified from a hybridoma clone producing human monoclonal antibody against CD4 at JNCASR was used for conjugation [30], Traut's reagent (2-iminothiolane) was procured from Sigma–Aldrich, USA, CellTiter 96® AQueous one solution was purchased from Promega, USA.

2.2. Preparation of dual drug loaded anti-CD4 conjugated immunoliposomes

The liposomes were prepared by the thin film hydration method [31,32]. The lipid combination of egg PC:cholesterol:DSPE–PEG of desired composition dissolved in chloroform was purged with nitrogen for removal of solvent and formation of a thin layer of lipid. This was followed by the addition of the hydrophobic drug nevirapine in chloroform and the solvent was removed by purging with nitrogen. Saquinavir dissolved in phosphate buffered saline (PBS) was added to the lipid–nevirapine layer for hydration. The mixture was constantly stirred at 60 °C for half an hour in a water bath followed by extrusion through a polycarbonate membrane with pore size of 0.2 μm to obtain unilamellar liposomes. The liposomes were then centrifuged at 845*g* (3000 rpm) to sediment the unencapsulated nevirapine [31]. The supernatant was then centrifuged at 21,130*g* (15,000 rpm) to sediment the dual drug loaded liposome. The supernatant containing the unencapsulated saquinavir was used to estimate the amount of drug encapsulated in the liposomes [32]. For conjugation of the anti-CD4 antibody to the dual drug loaded liposome was achieved in two steps. Initially, the antibody was thiolated using Traut's reagent with an antibody to reagent ratio of 1:20 (mol/mol) [33]. The reaction was carried out at room temperature for 1 h at pH 8. The unreacted Traut's reagent was removed by dialysis and the thiolated antibody was conjugated with the dual drug loaded liposomes by incubation overnight at 4 °C in HBS (HEPES buffer solution of pH 7.4) [34]. The unconjugated antibody was separated using Centriprep® (Millipore, India) at 9391 g (10,000 rpm). The amount of antibody conjugated to the liposome was estimated using the standard Lowry's method and the colored product obtained was read at 660 nm using multimode reader (Infinite M200, Tecan, Austria). The anti-CD4 conjugated immunoliposomes were freeze-dried (Alpha 2-4 LD *plus*, Christ, Germany) and stored in airtight moisture-free vials at −20 °C until further use.

2.3. Characterization of anti-CD4 conjugated immunoliposomes

Lyophilized unconjugated liposomes or anti-CD4 conjugated immunoliposomes (500 μg) were dispersed in 500 μL of PBS and placed over a copper grid. Then, PBS was removed using filter paper and the sample was allowed to dry followed by imaging using high resolution transmission electron microscopy (JEM 2100F, JEOL, Japan).

The amount of nevirapine and saquinavir encapsulated was determined from the amount of unencapsulated drugs. The unencapsulated nevirapine was pelletized by centrifugation of the extruded liposomes at 3000 rpm (Eppendorf 3340R, Germany).

The pellet was dissolved in methanol and the absorbance was measured at 284 nm using UV–visible spectrophotometer (Lambda 25, Perkin Elmer, USA). The supernatant was centrifuged at 15,000 rpm to sediment the dual drug loaded liposomes and the supernatant was analyzed at 239 nm to determine the amount of unencapsulated saquinavir. The absorbance values were converted to concentration using standard plots for nevirapine and saquinavir. The entrapment efficiency was calculated as follows:

$$\textit{Encapsulation efficiency} = \frac{\textit{Total drug} - \textit{Unencapsulted drug}}{\textit{Total drug}} \times 100$$

2.4. FTIR

The infrared spectra of the unconjugated liposomes, anti-CD4 conjugated immunoliposomes and free drugs were recorded using a FTIR spectrometer (Spectrum 100, PerkinElmer, USA). The samples were pelletized using KBr (IR grade, Merck, India) using a hydraulic press. The FTIR analysis was performed between 4000 and 400 cm^{-1} at a resolution of 1 cm^{-1} averaging 10 scans.

2.5. Particle size and zeta potential

The particle size of the blank and dual drug-loaded unconjugated liposomes and anti-CD4 conjugated immunoliposomes was measured using the laser diffraction method (Microtrac Blue wave, Nikkiso, Japan). About 500 μg of the sample dispersed in 1 mL of PBS was introduced in the flow channel and the average particle size was analyzed at the flow rate of 50%. The zeta potential of the samples was measured using the Zeta sizer (Nano-ZS, Malvern, UK). About 500 μg of the sample dispersed in 1 mL of the PBS was used for recording the zeta potential.

2.6. Thermal analysis

The phase transition temperatures of the blank and dual drug-loaded unconjugated liposomes and anti-CD4 conjugated immunoliposomes were determined using differential scanning calorimetry (DSC, Q20, TA Instruments, USA). Two mg of the sample was placed in an aluminum pan and the DSC was recorded between 10 °C and 100 °C in nitrogen atmosphere at a ramp rate of 10 °C per minute. Aluminum was used as the reference to determine the heat flow.

2.7. Colloidal stability

The colloidal stability of the liposomes was determined by measuring the particle size at pre-determined time intervals at 37 °C. About 30 mg of the liposomal sample was added in 100 mL of PBS supplemented with 10% FBS and incubated at 37 °C for different time intervals. The samples were withdrawn at regular intervals of time and the particle size was measured using the laser diffraction method (Microtrac Blue wave, Nikkiso, Japan).

2.8. Release kinetics

The *in vitro* drug release of nevirapine and saquinavir from the anti-CD4 conjugated immunoliposomes and unconjugated liposomes in PBS and in PBS containing 10% FBS (fetal bovine serum) was carried out. The lyophilized liposome samples were dispersed in 4 mL of PBS and taken in a dialysis bag sealed on both sides. The bag was placed in a release medium containing PBS and 10% methanol to achieve perfect sink conditions. The release medium was withdrawn at pre-determined time intervals to quantify the amount of drug released and replaced with fresh medium. The amount of drug released was determined by measuring the absorbance using a UV–visible spectrophotometer (Lambda 25, Perkin Elmer, USA) at 239 nm for saquinavir and 280 nm for nevirapine with appropriate controls. The absorbance was then converted to concentration using standard plots. The same procedure was followed for evaluating the stability of liposomal samples in the presence of protein where the release medium also contained 10% FBS solution in addition to PBS.

2.9. Evaluation of cell uptake of anti-CD4 conjugated immunoliposomes

The cell uptake of the unconjugated liposomes and anti-CD4 conjugated immunoliposomes was qualitatively assessed using laser scanning confocal microscopy (FV1000, Olympus, Japan) [35]. The liposomes were labeled with fluorescent NBD-conjugated lipids and loaded with the fluorophore Alexafluor 647 for visualization. Fifty thousand Jurkat T cells were suspended in 200 μL of RPMI medium and were incubated with the fluorescent liposomal samples. The cells were incubated at 37 °C in an incubator in 5% CO_2 for 15 min followed by addition of 200 μL of PBS supplemented with 5 μg of Hoechst 33258. The cells were then imaged using laser scanning confocal microscopy. For flow cytometry analysis, Jurkat T-cells, 0.5×10^5 cells were incubated in 200 μL of plain RPMI containing blank unconjugated liposomes or Alexafluor 647 loaded anti-CD4 conjugated immunoliposomes of concentration of lipid. The cells were incubated at 37 °C in 5% CO_2 incubator for 30 min and washed twice in 1× PBS. Cells were stained with Live/Dead Fixable Green Stain Kit (Molecular Probes, Invitrogen Detection Technologies, USA) for 30 min in dark as per manufacturer's instructions. Cells were washed twice in 1× PBS and fixed in 400 μL of 1% paraformaldehyde before acquisition using FACS Calibur flow cytometer. Data were analyzed using BD Cell Quest Pro software.

3. Evaluation of *in vitro* cytotoxicity

Cytotoxicity was evaluated *in vitro* for both unconjugated liposomes and anti-CD4 conjugated immunoliposomes with dual drugs loaded and blank liposomes in Jurkat T-cells using the MTS cell proliferation assay. Briefly, 2×10^4 cells in RPMI 1640 media were seeded in a 96-well flat-bottomed tissue culture plates. The cells were incubated at 37 °C in a 5% CO_2 incubator for 24 h. Appropriate concentrations of different liposomes suspended in PBS were added and the cells were incubated for 48 h. After incubation, the cells were washed with PBS and MTS assay was performed as per the manufacturer's instructions.

3.1. In vitro antiviral efficacy of dual drug-loaded anti-CD4 conjugated immunoliposomes

Human embryonic kidney HEK293T cells were grown in Dulbecco's modified Eagle's medium (Sigma–Aldrich, USA) supplemented with 10% heat inactivated fetal bovine serum (Biological Industries, Israel), 2 mM glutamine, 100 units/mL penicillin G, and 100 g/mL streptomycin. The Jurkat cells were cultured in RPMI 1640 medium (Sigma–Aldrich, USA) supplemented with 10% fetal bovine serum. All the cells were maintained at 37 °C in an incubator in the presence of 5% CO_2.

3.1.1. Production of the viral stocks

The viral stocks were prepared using HEK293T cells by transiently transfecting the cells with plasmid DNA containing the HIV-1 molecular clones NL4-3 (subtype B). Cells seeded in 100 mm dishes at a low confluency were transfected 24 h later

with 10 μg of the viral plasmid DNA. The culture medium was changed after 6 h of incubation and the culture supernatant containing the virus was harvested at 60 h, passed through a 0.45 μm filter and stored in multiple aliquots at −80 °C until use. The concentration of the viral core protein p24 in the viral stocks was measured using a commercial ELISA kit (Advanced BioScience Laboratories, USA) following the manufacturer's instructions. Viral stock of 10 ng p24 equivalent was used for the infection of Jurkat-T cell lines [36].

3.1.2. Viral inhibition assay

The *in vitro* viral inhibition was evaluated in Jurkat T-cell lines. The cells suspended in plain RPMI medium and seeded in 24-well culture plates, 0.5×10^6 per well, were exposed to five different concentrations (0, 5, 25, 125 and 625 ng/500 μL) of saquinavir (SQV) in the soluble form, five different concentrations (0, 6.2, 31.2, 156 and 780 ng/500 μL) of neviraprine (NVP) in the soluble form, five different concentrations of dual drug (SQV and NVP) loaded liposomes or soluble form of dual drug treatment (in dual drug treatment concentrations of the SQV and NVP drug is normalized to the single drug treatment). The total amount of liposome used in the experiment was normalized to 1260 ng and anti-CD4 conjugated immunoliposomes were normalized to 1660 ng using blank anti-CD4 conjugated immunoliposomes nanoparticles. Cells in 400 μL of plain medium were incubated for 30 min at 37 °C and in the presence of 5% CO_2. Following the incubation, Jurkat-T cells were infected with NL4-3 viruses, respectively, by adding 10 ng of p24 equivalent of the virus to appropriate wells. The final volume in each well was made up to 500 μL by adding complete medium supplemented with fetal bovine serum and DEAE dextran, the latter used at a final concentration of 8 μg/mL. Cells were incubated for 6 h, at 37 °C and in the presence of 5% CO_2. The cells were centrifuged at 2000 rpm and the cell pellet was washed three times with 500 μL of 1X PBS (pH 7.2). The cells resuspended in 1 mL of complete medium were incubated for 3 days at 37 °C in the presence of 5% CO_2. All the assays were performed in duplicate wells. The amount of viral antigen p24 secreted into the medium was monitored using a commercial kit (Advanced BioScience Laboratories, USA). 100 μL of cell-free supernatants of the infected cultures was harvested at 48 h and the frozen aliquots were stored in a deep freezer until the analysis. An unpaired two-tailed *t*-test was performed using the Graphpad Prism 5 software to determine the significance of differences in the magnitude of viral inhibition between the groups.

4. Results and discussion

4.1. Formation of anti-CD4 conjugated immunoliposomes

The conjugation of the anti-CD4 conjugated immunoliposomes was achieved through covalent linking of the thiolated antibody to maleimide terminated PEGylated lipid used to form the liposomes according to the following scheme represented in Fig. 1. Quantification of the amount of free antibody by Lowry's method revealed that about 75% of the antibody used for the reaction was conjugated to the liposome. The successful conjugation of the antibody was confirmed using FTIR spectroscopy.

4.2. Morphology of anti-CD4 conjugated immunoliposomes

The morphology of the liposome samples was investigated using transmission electron microscopy (Fig. 2). Both unconjugated liposomes and anti-CD4 conjugated immunoliposomes exhibited a nearly spherical morphology [37,38]. The transmission electron micrograph of the anti-CD4 conjugated immunoliposomes also reveals the presence of antibodies on the surface the anti-CD4 conjugated immunoliposomes. Further confirmation of the presence of antibodies on the surface of the anti-CD4 conjugated immunoliposomes was obtained through FTIR spectroscopy.

4.3. FTIR

The unconjugated liposomes showed a band at 2912 cm^{-1} due to the –C–H stretch of the methylene groups and a strong band at 1723 cm^{-1} due to the stretching vibration of the ester carbonyl. The $-CH_2-$ scissoring bend appears at 1465 cm^{-1} and the long chain band due to the $-CH_2-$ rocking appears around 738 cm^{-1}. The P–O stretch corresponding to the phosphate groups appears at 963 cm^{-1}. The FTIR spectrum of the anti-CD4 conjugated immunoliposomes displays a prominent broad band around 3400 cm^{-1} that may be attributed to the hydrogen bonded –OH stretching vibrations which is present in the PEG chains [39]. The characteristic bands due to the asymmetric stretch and symmetric stretch respectively of $-CH_2-$ appear at 2926 cm^{-1} and 2852 cm^{-1}. The corresponding scissoring vibrations were observed at 1464 cm^{-1}. The stretching vibration of the ester carbonyl is visible at 1736 cm^{-1}. The vibration of the P–O bond from the phospholipids appears at 934 cm^{-1}. The FTIR spectrum of the anti-CD4 conjugated immunoliposomes also exhibited several new bands. The strong band at 1643 cm^{-1} may be attributed to the stretching vibrations of the amide carbonyl group. The band at 635 cm^{-1} indicates the presence of a C–S bond (thioether bond) formed due to the covalent linking of the thiolated antibody to the maleimide terminal of the PEGylated lipid. The OH vibrations arise mainly due to the PEG moiety in DSPE-PEG lipid and from bound water. The new vibration band due to thioether linkage (C–S bond) at 635 cm^{-1} confirms the conjugation of the antibody with the malemide group of the liposome, which is absent in case of the unconjugated liposomes. Similar observations have been reported in earlier literature [40–42]. The strong vibration band at 1188 cm^{-1} may be attributed to the –C–O stretch from the PEG chain in the anti-CD4 conjugated immunoliposomes. Fig. 3 shows the FTIR spectra of the blank liposomes and blank anti-CD4 conjugated immunoliposomes.

4.4. Entrapment efficiency

The encapsulation of nevirapine and saquinavir in liposomes was attempted with different lipid compositions. The presence of both drugs in the liposome was confirmed using UV–visible spectroscopy. Fig. 4 shows the UV–visible spectra of the dual drug loaded liposomes, free nevirapine and saquinavir.

It was observed that the dual drug loaded liposomes exhibited two bands at 280 nm and 239 nm that correspond to the λ_{max} of nevirapine and saquinavir respectively. This confirms the presence of both drugs in the liposome. Table 1 shows the encapsulation efficiency of both drugs in liposomes along with the particle sizes and zeta potential. It was observed that the encapsulation efficiency of nevirapine in liposomes was greater than that of saquinavir. This may be attributed to the differences in the hydrophobicity of both drugs. Nevirapine is more hydrophobic and hence preferentially localizes in the hydrophobic region of the liposome that constitutes the major part of the liposome [43]. In the case of the saquinavir, owing to its lower hydrophobicity, it is mainly localized closer to the hydrophilic aqueous core and hence exhibits lower encapsulation in the liposomes when compared with nevirapine. The lipid composition was found to influence the amount of drug encapsulated. The encapsulation efficiency of the hydrophilic drug saquinavir shows only a slight increase with PEGylation ($p > 0.05$). However, the encapsulation efficiency of the hydrophobic nevirapine decreases significantly on PEGylation. Nearly 45% decrease was observed in the

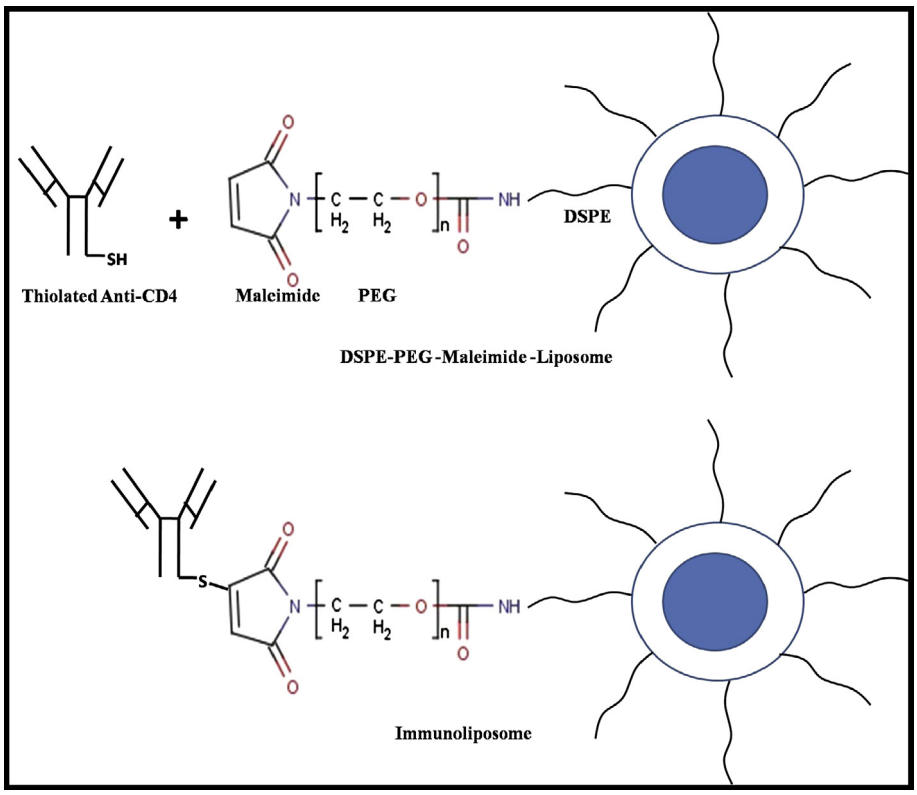

Fig. 1. Schematic representation of formation of anti-CD4 conjugated anti-CD4 conjugated immunoliposomes. (For interpretation of the references to color in this figure legend, the reader is referred to the web version of this article.)

encapsulation of nevirapine on introduction of PEG in the liposomes. The incorporation of cholesterol did not alter the encapsulation efficiency of saquinavir. But a significant increase in the encapsulation efficiency of nevirapine was observed in cholesterol containing liposomes [44]. The incorporation of PEG chains in the liposome enhances the hydrophilicity of the surface that may retard the partition of the hydrophobic nevirapine into the liposomes during the passive encapsulation process. In contrast, the incorporation of cholesterol contributes to the hydrophobicity as well as creates voids in the hydrophobic segment due to the acyl chain length mismatch [45]. This facilitates accommodation of more nevirapine molecules in the liposome. Presence of both cholesterol and PEG in equal proportions contributes equally in improving the encapsulation efficiency of both the hydrophobic nevirapine and hydrophilic saquinavir when compared with liposomes without cholesterol and PEG. Thus the ratio of 9:1:1 Egg PC:Chol:DSPE–PEG was found to be the best and hence used for further trials. The maximum entrapment efficiency for the hydrophobic drug nevirapine was 45% for nevirapine and 30% for saquinavir. Surface conjugation of the antibody on the liposome was not found to influence the encapsulation efficiencies of nevirapine and saquinavir significantly.

4.5. Particle size and zeta potential

Table 1 shows the particle size of the unconjugated liposomes and anti-CD4 conjugated immunoliposomes before and after encapsulation of the two drugs. The particle size of the anti-CD4 conjugated immunoliposomes was found to be larger than the unconjugated liposomes due to the additional layer of antibody on the surface. Other groups have also reported similar observations for antibody conjugated immunoliposomes [46]. The drug encapsulated liposomes exhibited larger size when compared to their blank counterparts. It was also observed that the amount of nevirapine in the liposomes influenced the particle size to a greater extent when compared to the amount of saquinavir. This may be due to the difference in the localization of the two drugs. While saquinavir is expected to localize preferentially closer to the aqueous core, nevirapine is localized in the hydrophobic regions that is reflected in the observed change in the particle size. The zeta potential of the unconjugated liposome and anti-CD4 conjugated immunoliposomes samples is negative due to the negatively charged phosphate groups in the phospholipids. Conjugation of antibody to the liposome leads to a slight positive shift in the zeta potential due to the masking of the surface charges on the liposome by the antibody. The PEG chains in the liposome shifts the zeta potential to the small extent but the presence of the antibody shifts the zeta potential to a larger extent due to its bulky nature that effectively masks the surface charges. In contrast, the PEG chains that are in constant motion expose the surface charges on the liposome for a longer duration when compared to the antibody [47]. The difference in the zeta potential of the blank and drug loaded liposomes also arises due to the masking of the surface charges by some drug molecules present in the surface as well as due to a decrease in the surface area leading to a decrease in the negative zeta potential [48,49]. The combined effect of increase in the hydrodynamic radius due to drug encapsulation and conjugation of the antibody on the liposomal surface contributes to the maximum positive shift observed in the drug loaded anti-CD4 conjugated immunoliposomes when compared to other combinations.

4.6. Thermal analysis

Fig. 5 shows the heat flow changes in the dual drug loaded anti-CD4 conjugated immunoliposomes compared with those in the anti-CD4 conjugated liposomes and free drugs. It was observed

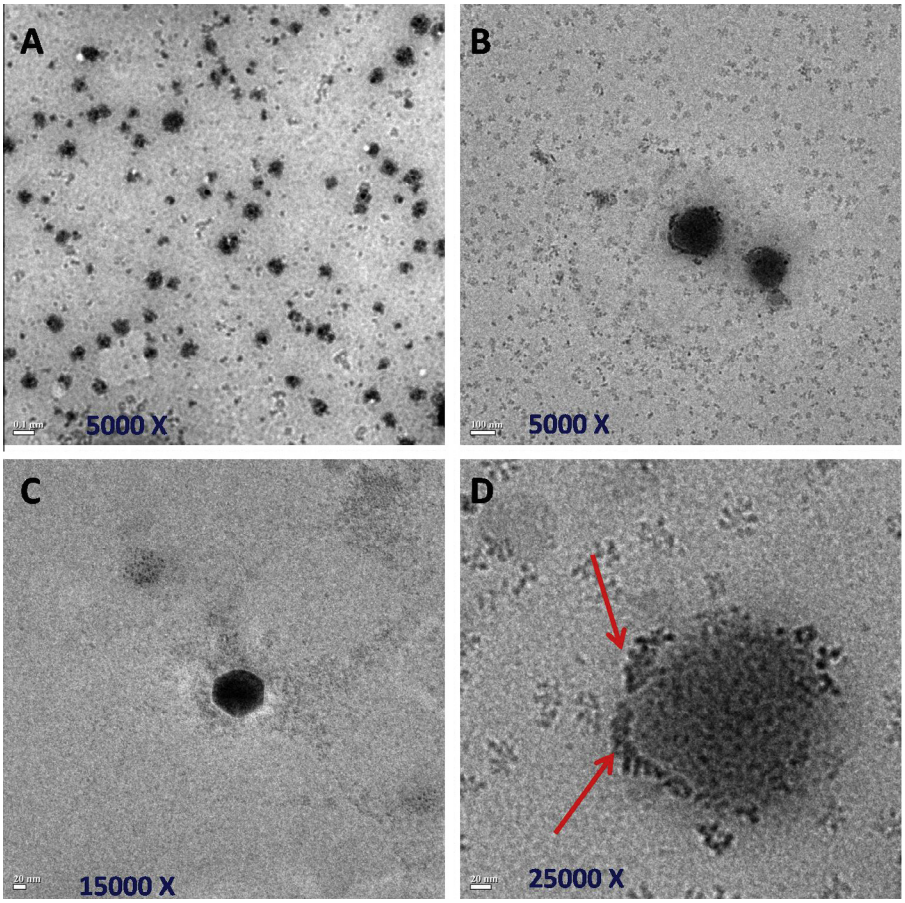

Fig. 2. Transmission electron micrographs of (A) and (C) Dual drug loaded PEGylated liposome, (B) and (D) Dual drug loaded anti-CD4 conjugated anti-CD4 conjugated immunoliposome. (For interpretation of the references to color in this figure legend, the reader is referred to the web version of this article.)

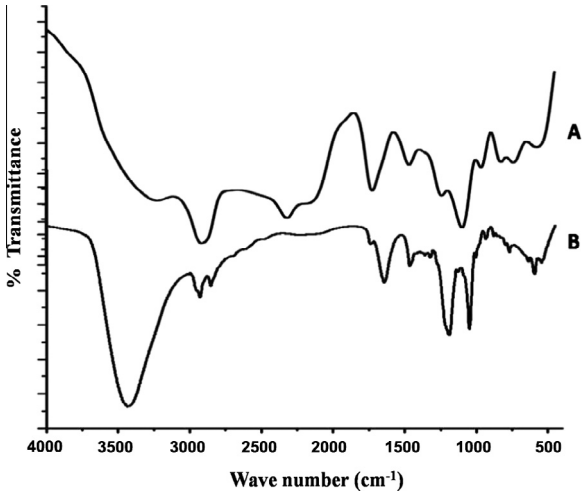

Fig. 3. FTIR spectra of (A) plain liposome and (B) anti-CD4 conjugated anti-CD4 conjugated immunoliposomes.

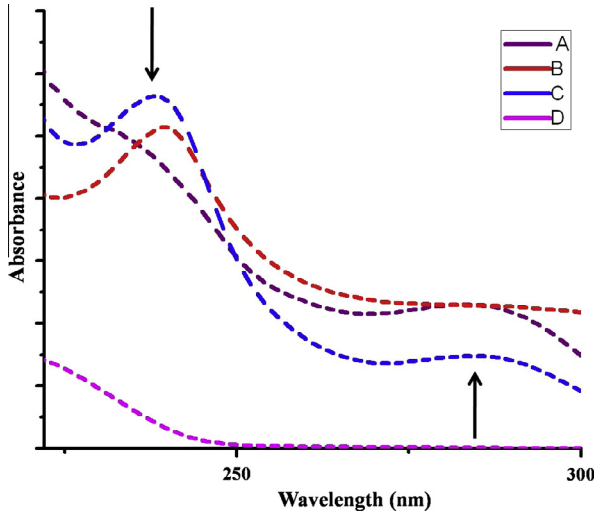

Fig. 4. UV–visible spectra of (A) free nevirapine, (B) free saquinavir and (C) dual drug loaded liposomes (D) Blank immunoliposomes. (For interpretation of the references to color in this figure legend, the reader is referred to the web version of this article.)

that the dual drug loaded anti-CD4 conjugated immunoliposomes exhibited four endothermic peaks. The peak at 46 °C corresponds to the phase transition of the phospholipids from the liquid crystalline phase to the gel phase while the peak at 112 °C corresponds to the melting curve of cholesterol [50]. The endothermic peaks at 226 °C and 254 °C correspond to the melting curves of nevirapine and saquinavir respectively. The differential scanning calorimetry confirms the presence of both drugs in the anti-CD4 conjugated immunoliposomes. The melting point of saquinavir in the liposome does not show any significant change when compared with the free drug. However, a small negative shift in the melting point

Table 1
Encapsulation efficiency, particle size and zeta potential of liposome with various lipid combinations.

Lipid composition	Encapsulation efficiency (%)		Particle size (nm)	Zeta potential (mV)
	Nevirapine	Saquinavir		
Egg PC (10:0)	42 ± 3	25 ± 3	149 ± 15	−19 ± 3
Egg PC:Chol (9:1)	55 ± 3	30 ± 1	189 ± 12	−23 ± 1
Egg PC:DSPE–PEG (9:1)	23 ± 2	28 ± 2	95 ± 8	−30 ± 1
Egg PC:Chol:DSPE–PEG (8:1:1)	40 ± 1	31 ± 2	122 ± 6	−31 ± 5
Egg PC:Chol:DSPE–PEG (9:1:1)	44 ± 2	30 ± 1	160 ± 2	−29 ± 2
Egg PC:Chol:DSPE–PEG-mal-anti-CD4 (9:1:1)	40 ± 1	29 ± 1	173 ± 7	−22 ± 1
Egg PC:Chol:DSPE–PEG (9:1:1) Blank	–	–	145 ± 2	−35 ± 1
Egg PC:Chol:DSPE–PEG-mal-anti-CD4 (9:1:1) Blank	–	–	150 ± 2	−32 ± 1

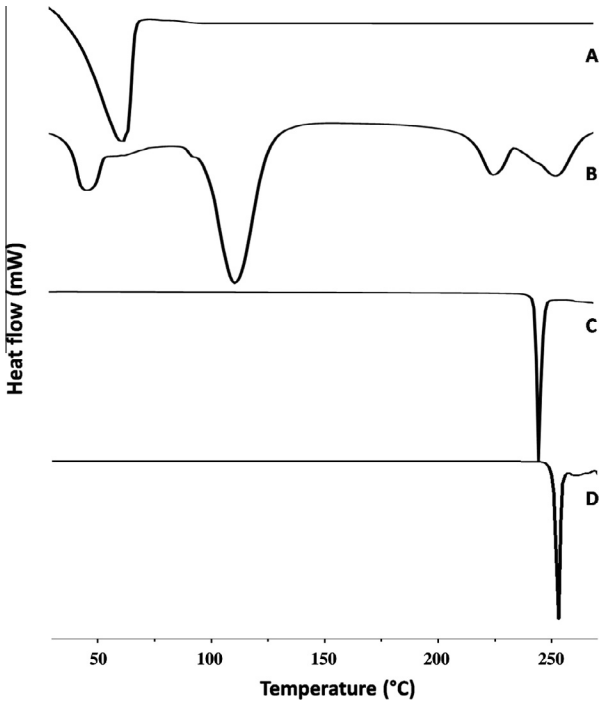

Fig. 5. Heat flow profiles of (A) Blank immunoliposomes (B) dual drug loaded anti-CD4 conjugated immunoliposomes; (B) free nevirapine and (C) free saquinavir.

curve of nevirapine in the liposome was observed when compared with the free drug. The endothermic heat flow recorded for nevirapine is broad instead of the sharp transition observed in the case of the free nevirapine. This indicates that nevirapine interacts with the phospholipid constituents of the liposomes. Similar observations have been reported for describing the interactions between verapamil and dextran [51]. The phase transition temperature (T_m) of the dual drug loaded anti-CD4 conjugated immunoliposomes was found to be higher than the T_m values recorded for the dual drug loaded liposomes (39 °C). A similar positive shift was observed in the case of blank anti-CD4 conjugated immunoliposomes (T_m = 63 °C) and blank liposomes (59 °C). This shift may be attributed to the covalently linked additional layer on the surface of the liposomes formed by the antibodies and PEGylated lipids. It was also observed that the encapsulation of both drugs in the anti-CD4 conjugated immunoliposomes resulted in a decrease of 27% in the phase transition temperature. This is because of the fluidity introduced in the acyl chains due to the incorporation of the drugs [52]. The dual drug loaded liposomes exhibit a corresponding decrease of about 34% in the phase transition temperature for the same reason. The greater magnitude of decrease observed in the unconjugated liposomes when compared with anti-CD4 conjugated immunoliposomes is due to the greater percentage of drugs encapsulated in the unconjugated liposomes resulting in a greater perturbation of the acyl chain packing.

4.7. In vitro release of nevirapine and saquinavir

Fig. 6A and B shows the release profiles of nevirapine and saquinavir from unconjugated liposomes and anti-CD4 conjugated immunoliposomes with PBS and 10% FBA as release medium. The release of saquinavir from PEGylated non-targeted liposomes over 30 min, 1 h and 2 h was 15%, 19% and 32% respectively. In comparison, the release of saquinavir from the immunoliposomes over the same time points of 30 min, 1 h and 2 h was 7%, 9.5% and 23% respectively. This represents a decrease in the release of saquinavir from immunoliposomes by 2.1-fold after 30 min, 2-fold after 1 h and 1.4-fold after 2 h when compared with its release at the same time points from PEGylated non-targeted liposomes. This decrease may be attributed to the additional layer of antibody present in the immunoliposomes [53,54]. In the case of nevirapine release also, a similar trend is observed. However, the magnitude of decrease is lesser in the case of nevirapine when compared to saquinavir. This is because burst release occurs due to drug molecules present closer to the surface of the liposome. Nevirapine being hydrophobic is localized in the lipid bilayer while saquinavir is predominantly localized in the interior aqueous core. Therefore, the difference in the drug release profiles from PEGylated non-targeted liposomes and immunoliposomes is more pronounced in the case of saquinavir than in nevirapine. Complete release of nevirapine and saquinavir was achieved in 28 h and 36 h respectively for nevirapine and saquinavir from the unconjugated liposomes and in 26 and 48 h respectively from the anti-CD4 conjugated immunoliposomes (Fig. 6A). The slower release observed in the anti-CD4 conjugated immunoliposomes may be attributed to the additional antibody layer on its surface that hinders the drug release. Similar observations have been reported in literature earlier [54,55].

Among the two drugs, saquinavir releases more slowly when compared with nevirapine. This difference may be due to the difference in the localization of the two drugs in the liposome. Nevirapine is closely associated with the acyl chains in the bilayer owing to its hydrophobic nature while saquinavir is expected to localize closer to the aqueous core. Hence it takes a longer time for saquinavir to diffuse from the interior of the liposomes to the exterior. The release profiles of the drugs from the liposomal carriers were fit in different kinetic models for drug release (Tables 2 and 3). It was observed that both nevirapine and saquinavir release profiles from anti-CD4 conjugated immunoliposomes and unconjugated liposomes agree well with the Korsmeyer–Peppas model suggesting that diffusion–swelling regime controls the extent of drug release from the liposomal carriers. The release exponent 'α' value was below 0.5 for nevirapine release in both PEGylated and anti-CD4 conjugated immunoliposomes indicating that the release follows a Fickian diffusion. However, the 'α' values for release of saquinavir from both unconjugated liposomes and anti-CD4

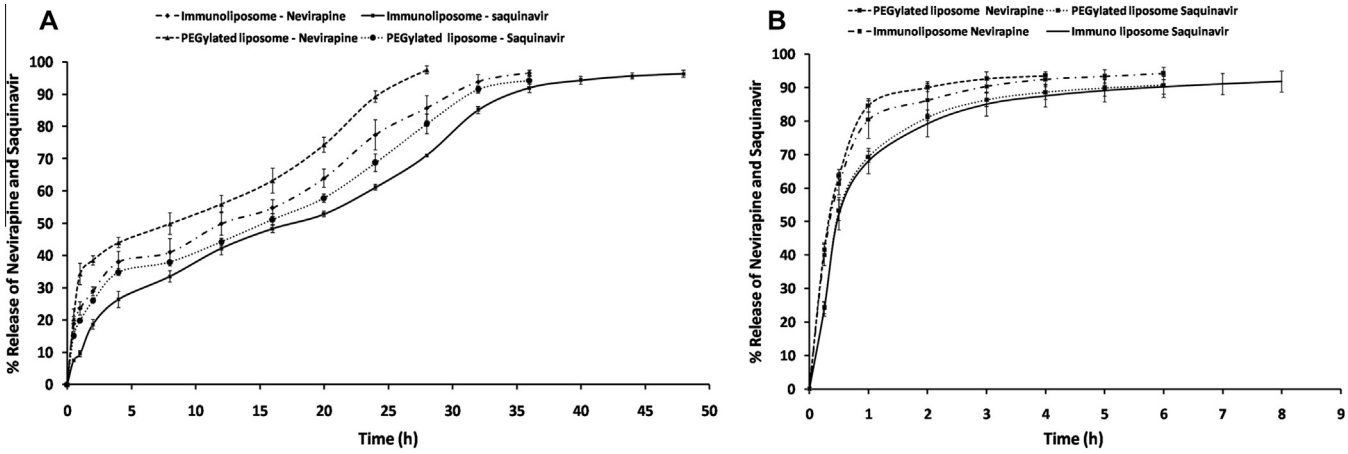

Fig. 6. *In vitro* release profile of nevirapine and saquinavir from PEGylated liposome and anti-CD4 conjugated anti-CD4 conjugated immunoliposomes in (A) PBS and (B) 10% FBS.

Table 2
Release kinetics model for dual drug release in PBS.

Kinetics model	PEGylated liposome Anti-CD4 conjugated anti-CD4 conjugated immunoliposomes							
	Nevirapine		Saquinavir		Nevirapine		Saquinavir	
	K	R^2	k	R^2	k	R^2	k	R^2
Zero order (k_0)	3.891	0.569	2.904	0.825	3.079	0.766	2.388	0.906
First order (k_1)	0.089	0.764	0.057	0.892	0.066	0.881	0.05	0.961
Higuchi model (k_H)	17.87	0.914	14.75	0.962	15.745	0.966	13.851	0.974
Korsmeyer–Peppas (k_{KP})	26.023	0.951 $\alpha = 0.366$	14.15	0.962 $\alpha = 0.513$	17.74	0.968 0.461	9.435	0.986 0.613
Hixson–Crowell (k_{HC})	0.023	0.721	0.015	0.886	0.017	0.868	0.013	0.969

conjugated immunoliposomes were above 0.5 indicating a non-Fickian diffusion [56].

The liposomal architecture is known to destabilize in the presence of proteins. Hence, the membrane integrity and stability of the liposomal carriers in protein medium was evaluated by monitoring the drug release in a medium containing 10% FBS (fetal bovine serum). As observed in phosphate buffered saline medium, the anti-CD4 conjugated immunoliposomes exhibit relatively slower release when compared with the unconjugated liposomes (Fig. 6B). However, the burst release as well as the time taken for complete release of the drugs is nearly fourfold more rapid in the protein-containing medium. This may be attributed to the disruption of the liposomal architecture through displacement of the phospholipids by the proteins in the medium [57]. The release kinetics of nevirapine and saquinavir from anti-CD4 conjugated immunoliposomes and unconjugated liposomes in protein-containing medium is found to agree with the Korsmeyer–Peppas model. The 'α' values in all cases were below 0.5 indicating a Fickian type of diffusional release from the liposomal carriers. The release of nevirapine from both anti-CD4 conjugated immunoliposomes and unconjugated liposomes also agree with the first order kinetics suggesting that the release of nevirapine is proportional to its concentration in the nanocarrier (Table 3). Saquinavir releases from the anti-CD4 conjugated immunoliposomes and unconjugated liposomes also follows the Baker–Lonsdale model indicating that the release is from a spherical matrix (Table 3) [56].

4.8. Colloidal stability

One of the challenges in the use of nanocarriers is their tendency to aggregate with time as a result of various factors such as masking of the surface charges by the ions in the medium, random collisions, fusion of nanoparticles and adsorption of proteins. PEGylation of liposomes has been reported to impart colloidal stability to the nanoparticles due to its ability to retard protein adsorption [58]. Fig. 7 shows the temporal variations in the particle size of the dual drug loaded unconjugated liposomes and anti-CD4 conjugated immunoliposomes. It was observed that the anti-CD4 conjugated immunoliposomes exhibited better colloidal stability when compared to the unconjugated liposomes up to 6 h. The enhanced steric repulsion between the particles due to the conjugation of the antibody to the liposome surface could have contributed to the improved colloidal stability in the case of anti-CD4 conjugated immunoliposomes [59,60].

4.9. Cell uptake of unconjugated liposomes and anti-CD4 conjugated immunoliposomes

The uptake of the unconjugated liposomes and anti-CD4 conjugated immunoliposomes by Jurkat T cells was evaluated qualitatively using laser scanning confocal microscopy and quantitatively using flow cytometry (Fig. 8A–C). To visualize the liposomes, they were formed using NBD-labeled lipids and were loaded with the fluorescent dye Alexa Fluor 647 (Fig. 8A). The confocal images recorded after 15 min show very good uptake of both unconjugated liposomes and anti-CD4 conjugated immunoliposomes by the cells (Fig. 8B). It is also evident that the distribution of the green fluorescent probe labeled anti-CD4 conjugated immunoliposomes is distinctly different from that observed in the unconjugated liposomes. The fluorescent anti-CD4 conjugated immunoliposomes were found to be localized on the surface of the cell membrane and are visible as bright intense spots

Table 3
Release kinetics of dual drugs in the presence of 10% FBS.

Kinetics model	PEGylated liposome Anti-CD4 conjugated anti-CD4 conjugated immunoliposomes							
	Nevirapine		Saquinavir		Nevirapine		Saquinavir	
	K	R^2	k	R^2	k	R^2	k	R^2
Zero order (k_0)	31.63	0.097	20.497	0.059	21.541	0.352	15.78	0.15
First order (k_1)	1.978	0.977	1.124	0.934	1.767	0.956	1.056	0.918
Higuchi model (k_H)	58.167	0.725	45.24	0.775	48.131	0.615	40.08	0.696
Korsmeyer–Peppas (k_{KP})	72.8	0.954 $\alpha = 0.230$	60.433	0.936 $\alpha = 0.271$	69.724	0.956 $\alpha = 0.202$	59.839	0.933 $\alpha = 0.242$
Hixson–Crowell (k_{HC})	0.362	0.85	0.23	0.839	0.248	0.719	0.178	0.773
Baker–Lonsdale (k_{BL})	0.125	0.942	0.083	0.947	0.083	0.887	0.062	0.924

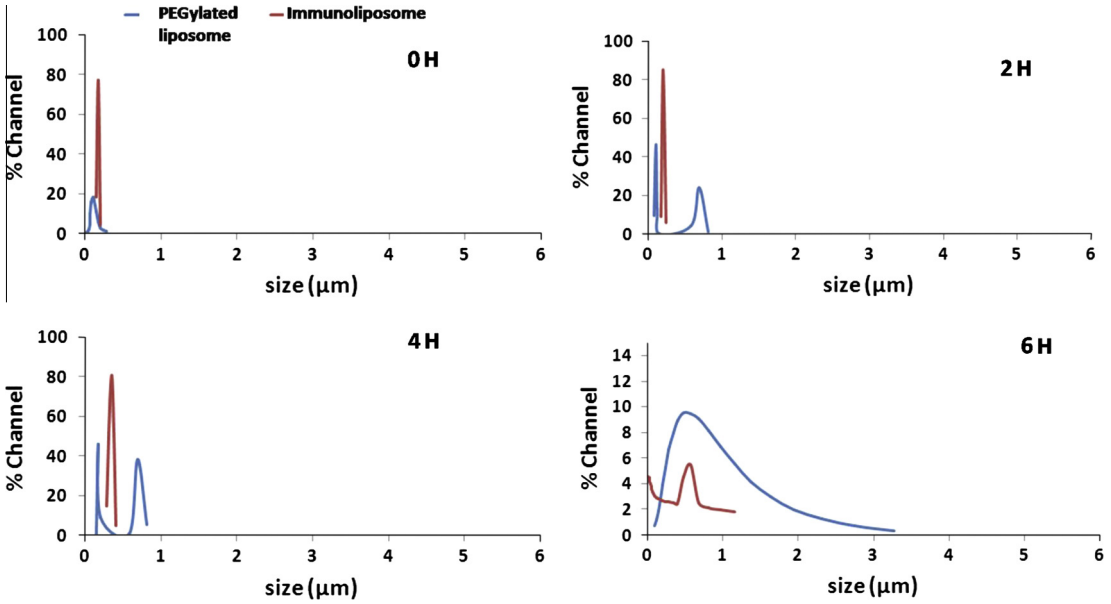

Fig. 7. Colloidal stability of PEGylated liposome and anti-CD4 conjugated anti-CD4 conjugated immunoliposomes supplemented with 10% FBS at various time points. (For interpretation of the references to color in this figure legend, the reader is referred to the web version of this article.)

indicating that the liposomes are bound with the target CD4 receptor. The binding with the receptor minimizes tumbling of the fluorescent molecule and hence its emission is bright. The unconjugated liposomes do not exhibit such intense emissions and are dispersed throughout the field suggesting that its mode of entry into the cells is not receptor-mediated. The appearance of red fluorescence inside the cells indicates that the liposomal carriers effectively delivered the fluorescent cargo into the cells. Quantification of the cell uptake using flow cytometry revealed a 54% uptake of the Unconjugated liposomes and a 98% uptake for the anti-CD4 conjugated immunoliposomes after 30 min but at a lower concentration (Fig. 8C) [61]. The difference in the uptake may be attributed to the presence of PEG chains at the liposomal surface in the unconjugated liposomes that hinders the uptake due to steric hindrance while in the case of the anti-CD4 conjugated immunoliposomes, the targeting moiety *i.e.*, anti-CD4 present in the distal end selectively binds to the CD4 receptors present in the surface of the Jurkat cells leading to efficient uptake through receptor-mediated endocytosis [62–65].

5. Evaluation of *in vitro* cytotoxicity

The *in vitro* cytotoxicity of the unconjugated liposomes and anti-CD4 conjugated immunoliposomes loaded with dual drugs is shown in Fig. 9. The drugs exhibited a dose-dependent cytotoxicity both in the free as well as liposomal form. At lower concentration of 0.5:0.62 µg of saquinavir and nevirapine, the toxicity is less when compared with those at higher concentration. The anti-CD4 conjugated immunoliposomes show higher toxicity at 20 µg due to its higher cellular uptake. The toxicity is lesser in case of the unconjugated liposomes and free dual drugs due to their lower uptake. The lower uptake in the unconjugated liposomes mainly arises due to the steric hindrance of the PEG chains on the surface of the liposome that inhibits the entry whereas in case of the free drugs nevirapine and saquinavir, the poor uptake may be attributed to their physicochemical properties.

5.1. In vitro antiviral efficacy of the liposomes

Considering the superior cell targeting properties of the anti-CD4 conjugated immunoliposomes nanoparticles, we examined if the anti-CD4 conjugated immunoliposomes could deliver anti-HIV drugs to target T-cells with a greater targeting efficiency since this could be beneficial by reducing the effective drug concentration required for comparable viral inhibition. Additionally, efficient drug delivery could also minimize the risk of drug resistance. We employed NL4-3, a subtype B molecular clone of HIV-1 in this assay. Cells in the group treated with the anti-CD4 conjugated immunoliposomes nanoparticle were exposed to an equal concentration of nanoparticle by using unconjugated liposomes or

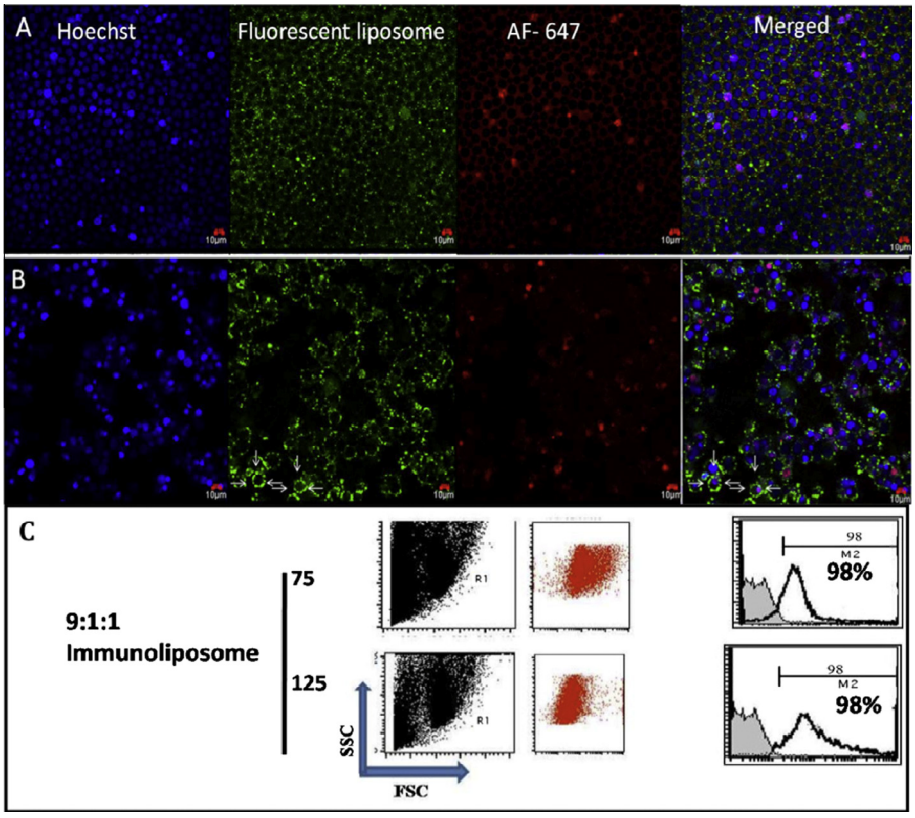

Fig. 8. Confocal image of (A) AF-647 loaded PEGylated fluorescent liposome and (B) AF-647 loaded fluorescent anti-CD4 conjugated anti-CD4 conjugated immunoliposomes. (C) Flow data for AF-647 loaded anti-CD4 conjugated anti-CD4 conjugated immunoliposomes. (For interpretation of the references to color in this figure legend, the reader is referred to the web version of this article.)

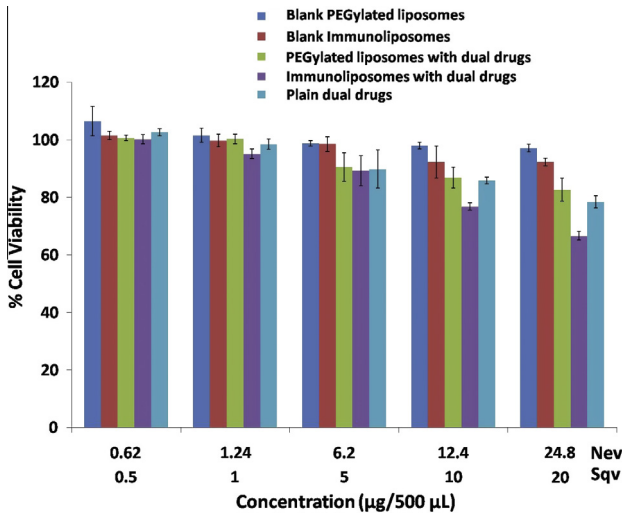

Fig. 9. Invitro cytotoxicity of PEGylated and anti-CD4 conjugated anti-CD4 conjugated immunoliposomes with dual drugs. (For interpretation of the references to color in this figure legend, the reader is referred to the web version of this article.)

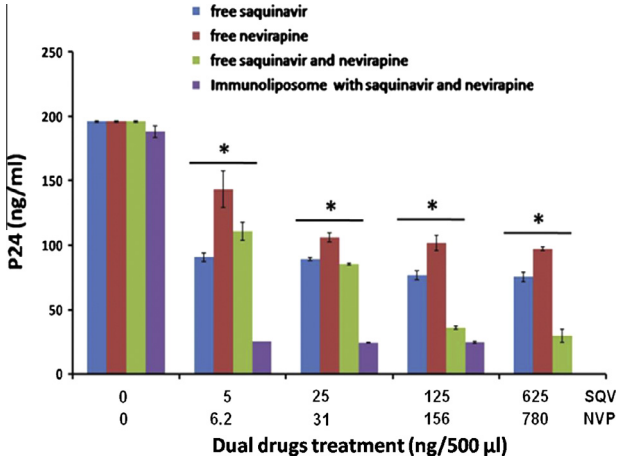

Fig. 10. Antiviral efficacy for dual drug loaded anti-CD4 conjugated anti-CD4 conjugated immunoliposomes. Jurkat T-cells were treated with five different concentrations of soluble SQV (blue bars), NVP (red bars), dual drugs (green bars) and dual drug loaded anti-CD4 conjugated anti-CD4 conjugated immunoliposomes (purple bars). In the anti-CD4 conjugated anti-CD4 conjugated immunoliposomes loaded drug treatment, the anti-CD4 conjugated anti-CD4 conjugated immunoliposomes concentration was normalized using blank anti-CD4 conjugated anti-CD4 conjugated immunoliposomes nanoparticles. Jurkat cells were infected with NL4-3 viruses respectively. The secretion of the viral antigen p24 into the medium was monitored using a commercial antigen-capture assay at 48 h following viral infection. An unpaired two-tailed t test was performed using Graphpad Prism 5 software to determine the significance of differences in the magnitude of viral inhibition. The results presented were obtained from two independent experiments with each experiment having $n = 4$. The standard deviations are for $n = 4$. (For interpretation of the references to color in this figure legend, the reader is referred to the web version of this article.)

anti-CD4 conjugated immunoliposomes nanoparticles for normalization. Saquinavir is a potent anti-retroviral agent that inhibits the viral protease efficiently and blocks viral maturation. On the other hand, neviraprine is a non-nucleoside reverse transcriptase inhibitor (NNRTI). We have studied viral inhibition by simultaneous dual drug treatment as well. T-cells in plain RPMI medium were first

treated by varying concentrations of soluble drug or with the nanoparticles loaded with an equivalent concentration of the drug (Fig. 10).

The single drug formulations were not as effective as the dual drug combination. In the case of the dual drug loaded anti-CD4 conjugated immunoliposomes, the p24 level seems to be four times reduced than the plain dual drug dosage at lower concentration of 7:5 ratio of nevirapine and saquinavir. In case of increasing the concentration the fold seems to be decrease from four to two folds. But in case of the higher dual drug dosage we can see that there is complete inhibition of the viral load, which is not observed in the case of the free dual drug dosage of the same concentration. Thus the targeting efficiency in the presence of the dual dosage shows the complete viral reduction at a concentration of 625 ng/mL of saquinavir.

6. Conclusions

Two anti-retroviral drugs were successfully loaded in a single nanocarrier and characterized for their physicochemical properties. The conjugation of anti-CD4 antibody enabled better uptake into CD4+ Jurkat cells. The use of both drugs simultaneously has shown better anti-viral efficacy at a lower concentration when compared with the individual drugs. The targeted nanocarrier further facilitates preferential delivery into HIV infected cells thereby reducing the dosage required for decreasing the viral load. The dual drug loaded anti-CD4 conjugated immunoliposomes exhibited better reduction of the p24 levels at much lower concentrations when compared to the free drugs indicating the potential of such targeted strategies in effectively reducing HIV load.

Conflict of interest

There is no conflict of interest.

Acknowledgments

The authors acknowledge financial support from ICMR (35/9/2009-BMS), FIST (SR/FST/LSI-453/2010), SASTRA University and JNCASR for infrastructural support.

Appendix A. Supplementary material

Supplementary data associated with this article can be found, in the online version, at http://dx.doi.org/10.1016/j.ejpb.2014.11.021.

References

[1] M.D. Hazenberg, D. Hamann, H. Schuitemaker, F. Miedema, T cell depletion in HIV-1 infection: how CD4+ T cells go out of stock, Nat. Immunol. 1 (2000) 285–289.
[2] B. Strong, The Marriage and Family Experience. Intimate Relationships in a Changing Society, Cengage Learning, 2013.
[3] S. Notari, A. Bocedi, G. Ippolito, P. Narciso, L.P. Pucillo, G. Tossini, R.P. Donnorso, F. Gasparrini, P. Ascenzi, Simultaneous determination of 16 anti-HIV drugs in human plasma by high-performance liquid chromatography, J. Chromatogr. B 831 (2006) 258–266.
[4] B. Peters, E. Carlin, R. Weston, S. Loveless, J. Sweeney, J. Weber, J. Main, Adverse effects of drugs used in the management of opportunistic infections associated with HIV infection, Drug Saf. 10 (1994) 439–454.
[5] Eagling, Profit, Back, Inhibition of the CYP3A4-mediated metabolism and P-glycoprotein-mediated transport of the HIV-1 protease inhibitor saquinavir by grapefruit juice components, Brit. J. Clin. Pharmacol. 48 (1999) 543–552.
[6] S. Dewhurst, K. Sakai, J. Bresser, M. Stevenson, M.J. Evinger-Hodges, D.J. Volsky, Persistent productive infection of human glial cells by human immunodeficiency virus (HIV) and by infectious molecular clones of HIV, J. Virol. 61 (1987) 3774–3782.
[7] D.R. Bangsberg, A.R. Moss, S.G. Deeks, Paradoxes of adherence and drug resistance to HIV antiretroviral therapy, J. Antimicrob. Chemother. 53 (2004) 696–699.
[8] V.K. Chaudhary, T. Mizukami, T.R. Fuerst, D.J. FitzGerald, B. Moss, I. Pastan, E.A. Berger, Selective killing of HIV-infected cells by recombinant human CD4-Pseudomonas exotoxin hybrid protein, Nature 335 (1988) 369–372.
[9] S. Dewhurst, J. Bresser, M. Stevenson, K. Sakai, M.J. Evinger-Hodges, D.J. Volsky, Susceptibility of human glial cells to infection with human immunodeficiency virus (HIV), FEBS Lett. 213 (1987) 138–143.
[10] T.K. Vyas, L. Shah, M.M. Amiji, Nanoparticulate drug carriers for delivery of HIV/AIDS therapy to viral reservoir sites, Expert Opin. Drug Deliv. 3 (2006) 613–628.
[11] L. Zhang, D. Pornpattananangkul, C.-M. Hu, C.-M. Huang, Development of nanoparticles for antimicrobial drug delivery, Curr. Med. Chem. 17 (2010) 585–594.
[12] P.N. Gupta, A. Pattani, R.M. Curran, V.L. Kett, G.P. Andrews, R.J. Morrow, A.D. Woolfson, R.K. Malcolm, Development of liposome gel based formulations for intravaginal delivery of the recombinant HIV-1 envelope protein CN54gp140, Eur. J. Pharm. Sci. 46 (2012) 315–322.
[13] E. Pedziwiatr-Werbicka, M. Ferenc, M. Zaborski, B. Gabara, B. Klajnert, M. Bryszewska, Characterization of complexes formed by polypropylene imine dendrimers and anti-HIV oligonucleotides, Colloids Surf., B 83 (2011) 360–366.
[14] Y.-C. Kuo, H.-F. Ko, Targeting delivery of saquinavir to the brain using 83–14 monoclonal antibody-grafted solid lipid nanoparticles, Biomaterials 34 (2013) 4818–4830.
[15] J. Meng, T.F. Sturgis, B.-B.C. Youan, Engineering tenofovir loaded chitosan nanoparticles to maximize microbicide mucoadhesion, Eur. J. Pharm. Sci. 44 (2011) 57–67.
[16] C. Destache, T. Belgum, K. Christensen, A. Shibata, A. Sharma, A. Dash, Combination antiretroviral drugs in PLGA nanoparticle for HIV-1, BMC Infect. Dis. 9 (2009) 1–8.
[17] A.A. Date, A. Shibata, M. Goede, B. Sanford, K. La Bruzzo, M. Belshan, C.J. Destache, Development and evaluation of a thermosensitive vaginal gel containing raltegravir + efavirenz loaded nanoparticles for HIV prophylaxis, Antiviral Res. 96 (2012) 430–436.
[18] U. Hengge, S. Esser, H.-P. Rudel, M. Goos, Long-term chemotherapy of HIV-associated Kaposi's sarcoma with liposomal doxorubicin, Eur. J. Cancer 37 (2001) 878–883.
[19] Y. Nishiyama, S. Karle, S. Planque, H. Taguchi, S. Paul, Antibodies to the superantigenic site of HIV-1 gp120: hydrolytic and binding activities of the light chain subunit, Mol. Immunol. 44 (2007) 2707–2718.
[20] K.B. Alexandre, E.S. Gray, B.E. Lambson, P.L. Moore, I.A. Choge, K. Mlisana, S.S.A. Karim, J. McMahon, B. O'Keefe, R. Chikwamba, L. Morris, Mannose-rich glycosylation patterns on HIV-1 subtype C gp120 and sensitivity to the lectins, Griffithsin, Cyanovirin-N and Scytovirin, Virology 402 (2010) 187–196.
[21] H. Yang, C. Lan, Y. Xiao, Y.-H. Chen, Antibody to CD14 like CXCR4-specific antibody 12G5 could inhibit CXCR4-dependent chemotaxis and HIV Env-mediated cell fusion, Immunol. Lett. 88 (2003) 27–30.
[22] J.-F. Gagné, A. Désormeaux, S. Perron, M.J. Tremblay, M.G. Bergeron, Targeted delivery of indinavir to HIV-1 primary reservoirs with immunoliposomes, Biochim. Biophys. Acta (BBA) – Biomembr. 1558 (2002) 198–210.
[23] T. Dutta, M. Garg, N.K. Jain, Targeting of efavirenz loaded tuftsin conjugated poly(propyleneimine) dendrimers to HIV infected macrophages in vitro, Eur. J. Pharm. Sci. 34 (2008) 181–189.
[24] V.A. Slepushkin, I.I. Salem, S.M. Andreev, P. Dazin, N. Düzgüneş, Targeting of liposomes to HIV-1-infected cells by peptides derived from the CD4 receptor, Biochem. Biophys. Res. Commun. 227 (1996) 827–833.
[25] O. Zelphati, G. Zon, L. Leserman, Inhibition of HIV-1 replication in cultured cells with antisense oligonucleotides encapsulated in immunoliposomes, Antisense Res. Dev. 3 (1993) 323–338.
[26] A.N. Endsley, R.J. Ho, Enhanced anti-HIV efficacy of Indinavir after inclusion in CD4 targeted lipid nanoparticles, J. Acquir. Immune Defic. Syndr. 61 (2012) (1999) 417.
[27] D. Flasher, K. Konopka, S.M. Chamow, P. Dazin, A. Ashkenazi, E. Pretzer, N. Düzgüneş, Liposome targeting to human immunodeficiency virus type 1-infected cells via recombinant soluble CD4 and CD4 immunoadhesin (CD4-IgG), Biochim. Biophys. Acta (BBA) – Biomembr. 1194 (1994) 185–196.
[28] E.M. Campbell, T.J. Hope, Live cell imaging of the HIV-1 life cycle, Trends Microbiol. 16 (2008) 580–587.
[29] M. Federico, HIV-protease inhibitors block the replication of both vesicular stomatitis and influenza viruses at an early post-entry replication step, Virology 417 (2011) 37–49.
[30] P.K. Dash, N.B. Siddappa, A. Mangaiarkarasi, A.V. Mahendarkar, P. Roshan, K.K. Anand, A. Mahadevan, P. Satishchandra, S.K. Shankar, V.R. Prasad, Exceptional molecular and coreceptor-requirement properties of molecular clones isolated from an Human Immunodeficiency Virus Type-1 subtype C infection, Retrovirology 5 (2008) 25.
[31] L.N. Ramana, S. Sethuraman, U. Ranga, U.M. Krishnan, Development of a liposomal nanodelivery system for nevirapine, J. Biomed. Sci. 17 (2010) 57.
[32] L.N. Ramana, S. Sharma, S. Sethuraman, U. Ranga, U.M. Krishnan, Investigation on the stability of saquinavir loaded liposomes: implication on stealth, release characteristics and cytotoxicity, Int. J. Pharm. 431 (2012) 120–129.
[33] T. Yang, M.-K. Choi, F.-D. Cui, J.S. Kim, S.-J. Chung, C.-K. Shim, D.-D. Kim, Preparation and evaluation of paclitaxel-loaded PEGylated immunoliposome, J. Control. Release 120 (2007) 169–177.
[34] M.R. Jafari, A.B. Jones, A.H. Hikal, J.S. Williamson, C.M. Wyandt, Characterization of drug release from liposomal formulations in ocular fluid, Drug Deliv. 5 (1998) 227–238.

[35] D. Sundaramurthi, U.M. Krishnan, S. Sethuraman, Biocompatibility of poly(3-hydroxybutyrate-co3-hydroxyvalerate)(PHBV) nanofibers for skin tissue engineering, J. Biomed. Nanotechnol. 9 (2013) 1383–1392.
[36] L.N. Ramana, S. Sharma, S. Sethuraman, U. Ranga, U.M. Krishnan, Evaluation of chitosan nanoformulations as potent anti-HIV therapeutic systems, Biochim. Biophys. Acta (BBA) – Gen. Sub. 1840 (2014) 476–484.
[37] X.-Y. Chen, S.-M. Wang, N. Li, Y. Hu, Y. Zhang, J.-F. Xu, X. Li, J. Ren, B. Su, W.-Z. Yuan, Creation of lung-targeted dexamethasone immunoliposome and its therapeutic effect on bleomycin-induced lung injury in rats, PLoS One 8 (2013) e58275.
[38] Z. Wang, J. Li, X. Xu, X. Duan, G. Cao, Urea immunoliposome inhibits human vascular endothelial cell proliferation for hemangioma treatment, World J. Surg. Oncol. 11 (2013) 300.
[39] M. Roberts, M. Bentley, J. Harris, Chemistry for peptide and protein PEGylation, Adv. Drug Deliv. Rev. 54 (2002) 459–476.
[40] S. Zalipsky, C.B. Hansen, D.E. Lopes de Menezes, T.M. Allen, Long-circulating, polyethylene glycol-grafted immunoliposomes, J. Control. Release 39 (1996) 153–161.
[41] J.W. Park, K. Hong, D.B. Kirpotin, D. Papahadjopoulos, C.C. Benz, Immunoliposome for cancer treatment, Adv. Pharmacol. 40 (1997) 399–435.
[42] C. Carrion, J. Domingo, M. De Madariaga, Preparation of long-circulating immunoliposomes using PEG–cholesterol conjugates: effect of the spacer arm between PEG and cholesterol on liposomal characteristics, Chem. Phys. Lipids 113 (2001) 97–110.
[43] S.L. Glynn, M. Yazdanian, In vitro blood–brain barrier permeability of nevirapine compared to other HIV antiretroviral agents, J. Pharm. Sci. 87 (1998) 306–310.
[44] I.V. Zhigaltsev, N. Maurer, Q.-F. Akhong, R. Leone, E. Leng, J. Wang, S.C. Semple, P.R. Cullis, Liposome-encapsulated vincristine, vinblastine and vinorelbine: a comparative study of drug loading and retention, J. Control. Release 104 (2005) 103–111.
[45] A.-T. Kuo, C.-H. Chang, Cholesterol-induced condensing and disordering effects on a rigid catanionic bilayer: a molecular dynamics study, Langmuir 30 (2013) 55–62.
[46] E. Markoutsa, G. Pampalakis, A. Niarakis, I.A. Romero, B. Weksler, P.-O. Couraud, S.G. Antimisiaris, Uptake and permeability studies of BBB-targeting immunoliposomes using the hCMEC/D3 cell line, Eur. J. Pharm. Biopharm. 77 (2011) 265–274.
[47] A.M. Robinson, J.E. Creeth, M.N. Jones, The specificity and affinity of immunoliposome targeting to oral bacteria, Biochim. Biophys. Acta (BBA) – Biomembr. 1369 (1998) 278–286.
[48] J. Gao, W. Liu, Y. Xia, W. Li, J. Sun, H. Chen, B. Li, D. Zhang, W. Qian, Y. Meng, L. Deng, H. Wang, J. Chen, Y. Guo, The promotion of siRNA delivery to breast cancer overexpressing epidermal growth factor receptor through anti-EGFR antibody conjugation by immunoliposomes, Biomaterials 32 (2011) 3459–3470.
[49] M. Ionov, Z. Garaiova, I. Waczulikova, D. Wróbel, E. Pędziwiatr-Werbicka, R. Gomez-Ramirez, F.J. de la Mata, B. Klajnert, T. Hianik, M. Bryszewska, siRNA carriers based on carbosilane dendrimers affect zeta potential and size of phospholipid vesicles, Biochim. Biophys. Acta (BBA) – Biomembr. 1818 (2012) 2209–2216.
[50] C.R. Loomis, G.G. Shipley, D.M. Small, The phase behavior of hydrated cholesterol, J. Lipid Res. 20 (1979) 525–535.
[51] Y. Li, N. Taulier, A. Rauth, X. Wu, Screening of lipid carriers and characterization of drug–polymer–lipid interactions for the rational design of polymer–lipid hybrid nanoparticles (PLN), Pharm. Res. 23 (2006) 1877–1887.
[52] D. Bilge, N. Kazanci, F. Severcan, Acyl chain length and charge effect on Tamoxifen–lipid model membrane interactions, J. Mol. Struct. 1040 (2013) 75–82.
[53] T.M. Allen, E. Brandeis, C.B. Hansen, G.Y. Kao, S. Zalipsky, A new strategy for attachment of antibodies to sterically stabilized liposomes resulting in efficient targeting to cancer cells, Biochim. Biophys. Acta (BBA) – Biomembr. 1237 (1995) 99–108.
[54] W. Huang, J. Zhang, H.C. Dorn, C. Zhang, Assembly of bio-nanoparticles for double controlled drug release, PLoS One 8 (2013) e74679.
[55] U.K. Nassander, P.A. Steerenberg, W.H. De Jong, W.O.W.M. Van Overveld, C.M.E. Te Boekhorst, L.G. Poels, P.H.K. Jap, G. Storm, Design of immunoliposomes directed against human ovarian carcinoma, Biochim. Biophys. Acta (BBA) – Biomembr. 1235 (1995) 126–139.
[56] S. Dash, P.N. Murthy, L. Nath, P. Chowdhury, Kinetic modeling on drug release from controlled drug delivery systems, Acta Pol. Pharm. 67 (3) (2010) 217–223.
[57] H.D. Han, B.C. Shin, H.S. Choi, Doxorubicin-encapsulated thermosensitive liposomes modified with poly(N-isopropylacrylamide-co-acrylamide): drug release behavior and stability in the presence of serum, Eur. J. Pharm. Biopharm. 62 (2006) 110–116.
[58] F. Zhang, E.T. Kang, K.G. Neoh, P. Wang, K.L. Tan, Surface modification of stainless steel by grafting of poly(ethylene glycol) for reduction in protein adsorption, Biomaterials 22 (2001) 1541–1548.
[59] M. Mercadal, J. Domingo, J. Petriz, J. Garcia, M. De Madariaga, A novel strategy affords high-yield coupling of antibody to extremities of liposomal surface-grafted PEG chains, Biochim. Biophys. Acta (BBA) – Biomembr. 1418 (1999) 232–238.
[60] M. Canovi, E. Markoutsa, A.N. Lazar, G. Pampalakis, C. Clemente, F. Re, S. Sesana, M. Masserini, M. Salmona, C. Duyckaerts, The binding affinity of anti-Aβ1-42 MAb-decorated nanoliposomes to Aβ1-42 peptides *in vitro* and to amyloid deposits in post-mortem tissue, Biomaterials 32 (2011) 5489–5497.
[61] K. Khantasup, P. Kopermsub, K. Chaichoun, T. Dharakul, Targeted small interfering RNA-immunoliposomes as a promising therapeutic agent against highly pathogenic avian influenza A (H5N1) virus infection, Antimicrob. Agents Chemother. 58 (2014) 2816–2824.
[62] U.B. Nielsen, D.B. Kirpotin, E.M. Pickering, K. Hong, J.W. Park, M. Refaat Shalaby, Y. Shao, C.C. Benz, J.D. Marks, Therapeutic efficacy of anti-ErbB2 immunoliposomes targeted by a phage antibody selected for cellular endocytosis, Biochim. Biophys. Acta (BBA) – Mol. Cell Res. 1591 (2002) 109–118.
[63] A. Okamoto, T. Asai, H. Kato, H. Ando, T. Minamino, E. Mekada, N. Oku, Antibody-modified lipid nanoparticles for selective delivery of siRNA to tumors expressing membrane-anchored form of HB-EGF, Biochem. Biophys. Res. Commun. (2014).
[64] M. Sioud, RNAi therapy: antibodies guide the way, Gene Ther. 13 (2005) 194–195.
[65] K.K. Matthay, A.M. Abai, S. Cobb, K. Hong, D. Papahadjopoulos, R.M. Straubinger, Role of ligand in antibody-directed endocytosis of liposomes by human T-leukemia cells, Cancer Res. 49 (1989) 4879–4886.